

Section III. Research instrumentation: (c) Detectors

DEVELOPMENTS IN GAS DETECTORS FOR SYNCHROTRON X-RAY RADIATION *

J. FISCHER, V. RADEKA, and G.C. SMITH

Brookhaven National Laboratory, Upton, New York 11973-5000, USA

New results on the physical limitations to position resolution in gas detectors for X-rays ($\approx 3\text{--}20\text{ keV}$) due to the range of photoelectrons and Auger electrons are discussed. These results were obtained with a small gap detector in which position readout was accomplished by using a very low noise centroid finding technique.

A description is given of position sensitive detectors for medium rates (a few $\times 10^5$ photons per second), using delay line readout, and for very high rates ($\approx 10^8$ photons per second), using fast signal shaping on the output of each anode wire.

1. Introduction

The increasing flux of photons available from synchrotron sources requires radiation detectors with greater and greater dynamic range in counting rate capability. It is usually the experimenter's wish that position resolution is not compromised at these higher counting rates. There exists quite a variety of position sensitive photon detectors, such as proportional counters, solid state detectors, scintillation detectors, and TV based detectors.

We give here an account of the present level of performance of position sensitive detectors which are based on the proportional counter, with particular reference to position resolution and counting rate. Results are presented which illustrate the fundamental limit to position resolution in a gas due to photoelectron range. There exists little accurate data in the literature on this particular limit and some of the results presented here are either very recent or new. In addition we have observed the effects on resolution of the fluctuations of the avalanche along the anode wire as a function of both the gas pressure and the avalanche size.

A brief description is given of position sensitive detectors using delay line readout, where it is seen that the resolution attainable is, in some cases, close to the photoelectron range limit.

Finally we describe a position sensitive proportional counter which is capable of operating at counting rates in excess of 10^8 s^{-1} . This is based on the "readout per wire" concept, and involves the optimization of several detector and electronic parameters in order to achieve such a count rate capability in single photon counting mode.

2. Physical limits to position resolution in gas

We are concerned here with X-rays in the energy range of about 3 to 20 keV. A photon passes through the detector window and is absorbed in the gas of the detector via the photoelectric effect. A photoelectron of energy ($E_X - E_B$) is created, where E_X is the X-ray energy and E_B is the binding energy of the electron shell in which the X-ray interacts. De-excitation of the absorbing atom occurs by emission of either an Auger electron or a fluorescent photon, depending upon the Z of the gas and the X-ray energy. In cases where fluorescence emission occurs with low probability, the gas in the vicinity of the absorbing atom is ionized by the photoelectron and Auger electron until both electrons thermalize. It is the finite spatial extent of this ionization which determines the ultimate position line width ("point spread function") of the detector.

We have reported earlier [1] the general behavior of position resolution with X-ray energy in methane, argon, and xenon. In hydrocarbons, such as methane, where X-rays interact in the carbon K shell (binding energy 0.28 keV) nearly all the X-ray energy is converted into kinetic energy of the photoelectron. The electron range has approximately an $E^{1.8}$ dependence (where E = electron energy), and therefore the position line width also increases as a similar power law relationship with X-ray energy. In argon (K shell binding energy = 3.2 keV) and xenon (average L shell binding energy ≈ 5 keV) the emission of an Auger electron from the X-ray absorbing atom, when the X-ray energy is above the respective electron shell binding energy, results in significantly improved localization of the X-ray absorption point [1]. Only when the X-ray energy is ≈ 10 keV or greater does the range of the photoelectron begin to dominate over the range of the Auger electron and resolution starts approaching an $E_X^{1.8}$ dependence again (see fig. 3, ref. [1]).

* This research was supported by the U.S. Department of Energy: Contract No. DE-AC02-76CH00016.

In normal operation of physically large detectors other factors also contribute to the position line width, most importantly electronic noise and diffusion of electrons during their drift in the gas. We have built a special detector system shown in fig. 1, which is designed to reduce the magnitude of both these effects to a level which is small compared with that of photoelectron range. This is achieved primarily by using a very low noise readout system and a very thin detector [2]. Each readout strip on the cathode is connected to a low noise charge sensitive preamplifier, followed by a shaping amplifier with approximately $2 \mu\text{s}$ time constant, and a sample and hold. After an X-ray event has been detected (as signified by a prompt anode signal) the sampled signal from each cathode channel is sequentially switched, under control from a fast clock, into a centroid finding filter [3,4]. An example of the input to the filter, generated by this switching, is shown by the oscilloscope traces in fig. 1, which are due to X-rays

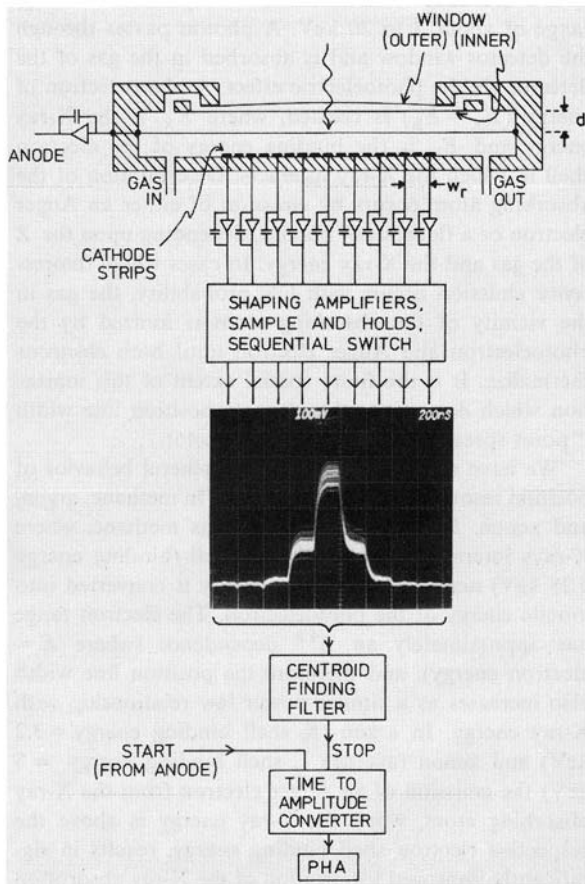


Fig. 1. Schematic diagram of gas proportional chamber for studies of electron range effects, and the essential features of the position readout electronics. Half-gap, d , of chamber = 0.8 mm, cathode strip pitch = 0.575 mm, readout pitch, w_r = 1.15 mm.

entering the detector exactly above the center of a readout strip. These waveforms spatially represent the quasi-Lorentzian shape of induced cathode charge. The time centroid of these waveforms is measured by the linear centroid finding filter, which has the required property of including signal and noise only from outputs containing centroid information, thereby minimizing line width broadening due to electronic noise. The timing signal which represents the centroid provides a stop signal for the time-to-amplitude converter (TAC) to which a start signal (delayed by up to one clock period to produce synchronization with the clock) is applied from the anode channel. A pulse height analyzer (PHA) records the signals from the TAC. In actual detector systems this time is digitized by using the same clock from which the controls signals for the sequential switch are derived [3].

The criteria by which the choice of clock frequency and strip pitch are chosen, in order to produce a system with good position linearity and minimum electronic noise, are beyond the scope of this paper, and are treated more fully in refs. [2] and [4]. We now describe some results of position resolution measurements with this set-up.

2.1. 8 keV X-rays in xenon

Fig. 2(a) shows position resolution vs anode charge for 8 keV X-rays (Cu K_α) in Xe/10%CO₂ at 1, 2 and 5

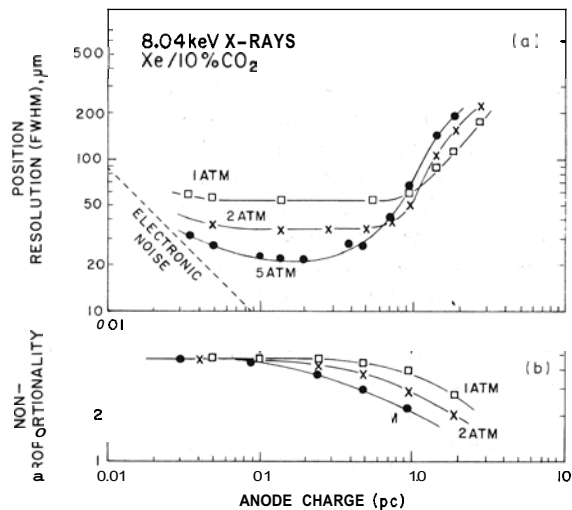


Fig. 2(a) Position resolution (fwhm) vs anode charge (as measured in $1 \mu\text{s}$) for 8 keV X-rays in various pressures of Xe/10%CO₂. (X-ray beam width $\approx 15 \mu\text{m}$.) (b) Nonproportionality of gas detector vs anode charge with various pressures of Xe/10%CO₂. Ordinate is the ratio of most probable pulse height for 8 keV X-rays to that of the escape peak from 5.9 keV X-rays (8 keV: 1.7 keV).

atm (absolute pressure). At 1 atm there is a plateau of resolution at $\approx 60 \mu\text{m}$ fwhm, which represents the limit due to photoelectron and Auger electron range (fig. 3, ref. [1]). At 2 atm the value of the plateau region is about half the resolution corresponding to that at 1 atm, while at 5 atm there is really no plateau, just a minimum of resolution. At all three pressures, resolution deterioration occurs at low charge levels because of electronic noise. At high charge levels there is a deterioration which is associated with photon mediated avalanche growth along the anode wire, such as photoionization of the surrounding gas or photoemission from the cathodes. The deterioration in position resolution which occurs with increasing anode charge is accompanied by degradation in two other properties of the gas proportional counter. These are nonproportionality and energy resolution. Fig. 2(b) shows nonproportionality as a function of anode charge for the three gas pressures used.

The charge level at which resolution begins to deteriorate exhibits an inverse relationship with gas pressure. Thus at 5 atm the electron range limited resolution is probably not quite reached since there is no well defined plateau of resolution. The operation of proportional counters at high charge levels results in both a decrease in detector lifetime because of the formation of deposits on the anode wire, and an increased susceptibility to space charge effects at high counting rates. The curves in fig. 2 clearly demonstrate that the position resolution capability can be degraded at high charge levels, particularly as the operating gas pressure is increased.

The minimum position resolution measured for 8 keV X-rays in 5 atm Xe/10%CO₂ is 22 μm fwhm – this is considerably better than has ever been reported for a gas detector and is comparable with the pixel size of silicon photodiodes and charge coupled devices (CCDs).

2.2. 17.4 keV X-rays in krypton

The problem of detecting, with reasonably high efficiency, X-rays of energy between about 10 and 20 keV can be addressed by the use of detectors with 4 or 5 atm of xenon. If position resolution of the order 100 μm is required, it is necessary, anyway, to use this kind of pressure to reduce the photoelectron range [1]. Krypton can give superior position resolution to xenon at X-ray energies a few keV above the krypton K edge (14.3 keV). We illustrate this point with some recent measurements [5] we have made using 17.4 keV X-rays (Mo K_α) in 1 atm. Kr/10%CO₂ for which fig. 3 shows the anode pulse height spectrum. The photopeak and escape peaks are due to direct interactions of the X-rays in the gas. Some X-rays pass straight through the gas and are absorbed in the rear copper cathode of the detector, creating Cu K fluorescence emission. The fluorescence

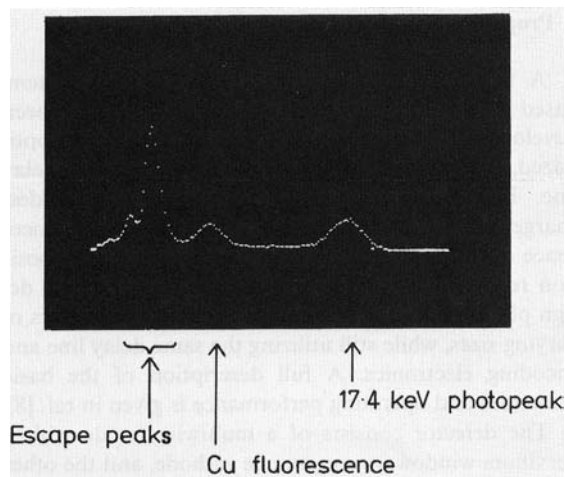


Fig. 3. Anode pulse height spectrum for 17.4 keV X-rays in 1 atm Kr/10%CO₂. Escape peaks are due to escape from the detector of K_α (12.6 keV) and K_β (14.1 keV) fluorescent photons.

peak in fig. 3 could be eliminated by using a different cathode material such as aluminum.

Anode signals recorded in the escape peaks correspond to X-ray interactions in the krypton K shell, and in which the krypton atom de-excites by fluorescence emission. The fluorescent photons (K_α, 12.6 keV or K_β, 14.1 keV) – nearly always escape from the thin detector because of their long range ($\approx 100 \text{ mm}$ in Kr/10%CO₂ at NTP). This leaves a photoelectron of energy 3.1 keV (since the K shell binding energy is 14.3 keV) which has a small range and the position information is very good. Photopeak events, on the other hand, comprise either X-ray interactions in the K shell where de-excitation has occurred via Auger emission (primary Auger electron energy $\sim 10.7 \text{ keV}$) or X-ray interactions in the krypton L shell (binding energy = 1.8 keV). Both types of interaction result in the production of one electron with a large range, and therefore poorer position information than for escape peak events.

We have measured the position resolution of escape peak events, and photopeak events, by gating the PHA of fig. 1 with the appropriate energy signal from the anode. At atmospheric pressure we obtain 80 μm fwhm and 580 μm fwhm, respectively, i.e., the escape peak events contain dramatically more accurate position information than photopeak events. It should be noted that by selecting only escape peak events, $\approx 56\%$ of all incoming X-rays absorbed in the gas are obtained.

The technique of obtaining good position resolution for X-ray energies just above the K edge energy has been reported for xenon, (K edge energy = 34.6 keV) using 42 keV X-rays, in a biomedical application [6,7]. The best measured resolution obtained in that case was approximately 0.5 mm.

III(c). DETECTORS

3. Proportional counters with delay line readout

A linear, position sensitive X-ray detector system, based on the multiwire proportional chamber, has been developed for some time at Brookhaven, using an optimized, low noise, position readout based on a delay line. This allows the chamber to operate at modest charge levels, which extends detector lifetime, reduces space charge effects, and is less likely to degrade position resolution, as explained earlier. An important design philosophy was the ability to construct detectors of varying sizes, while still utilizing the same delay line and encoding electronics. A full description of the basic principles and operating performance is given in ref. [8].

The detector consists of a multiwire anode with a beryllium window serving as one cathode, and the other cathode is in the form of conducting strips which allow position readout of the induced charge. The detector geometry is designed to yield good position resolution and linearity, high detection efficiency, low operating voltage (≈ 2 kV). In a detector with a 10×2 cm² collecting area, for example, anode-cathode spacing, $d = 33$ mm, anode wire pitch, $s = 32$ mm, cathode strip pitch, $w = 25$ mm. For larger (or smaller) detectors these dimensions are scaled appropriately. Good linearity is achieved by using $w/d \approx 0.75$ or less, and low operating voltage is obtained by allowing $s \approx d$. The cathode comprises 40 strips which couple directly into a lumped component delay line via an appropriate fan-out or fan-in board (depending upon the length of the detector). The 40 tap delay line is external to the detector with an impedance of 500Ω or 300Ω for total propagation times, T_D , of $1 \mu\text{s}$ or $0.5 \mu\text{s}$, respectively. As is usual with delay line detectors the position, x , of an event along the detector of length, l , is related to t_1 and t_2 , the times of the propagating charge signal to reach each end of the line, by

$$(t_1 - t_2)/T_D = 1 - 2x/l.$$

A low noise charge sensitive preamplifier correctly terminates each end of the delay line, and feeds a double delay line clipping amplifier whose zero cross time provides a measure of t_1 (and t_2). For routine bench testing these timing signals feed a TAC whose output is analyzed by a PHA. The typical resolution performance is shown in fig. 4, in which position resolution is plotted against anode charge, Q_A , for 5.41 keV X-rays in Ar/20%CO₂ and Xe/10%CO₂, for the 10×2 cm² chamber with $1 \mu\text{s}$ delay line. The position line width varies inversely with anode charge in the region where the electronic noise of the position readout dominates. (The noise and position resolution performance of the centroid finding system described in sect. 2 is much better, but at the expense of a more complex electronic readout system.) For a given anode charge, the position line width in xenon is worse than in argon

because the slower positive ion mobility of xenon, relative to argon, results in a smaller signal and a larger timing error, and hence a poorer effective signal to noise ratio. At higher anode charges, both curves tend to a plateau of resolution which is due primarily to the photoelectron range limited resolution ($\approx 100 \mu\text{m}$ in argon and $\approx 70 \mu\text{m}$ in xenon [1]).

The basic attributes of this type of delay line detector are:

- position resolution ≈ 100 pm, or 1 part in 10^3 ;
- integral nonlinearity of $\approx \pm 0.1\%$;
- differential nonlinearity $\pm 2\%$;
- counting rate capability $\approx 2 \times 10^5 \text{ s}^{-1}$;
- efficiency greater than 50% for energy range 3–20 keV (with use of 4–5 atm pressure for X-ray energies > 10 keV);
- detectors with 6 to 18 cm in length and 1 to 10 cm in width.

A new time-to-digital encoder based on direct time conversion has been developed at Brookhaven [9] in order to use effectively the counting rate capability of these detectors. The timing signals, t_1 and t_2 , from each end of the delay line, are used as stop signals for a fast digital clock (500 MHz) which has been started by an anode signal. After receiving the second stop signal, the encoder is reset, ready for analysis of the next event, within a time of only 75 ns. We have recently constructed detectors with $0.5 \mu\text{s}$ propagation time delay lines in order to increase the count rate capability (with correspondingly reduced resolution performance). The use of a fast digital encoder then becomes critically important. Delay line times down to $0.25 \mu\text{s}$ are also

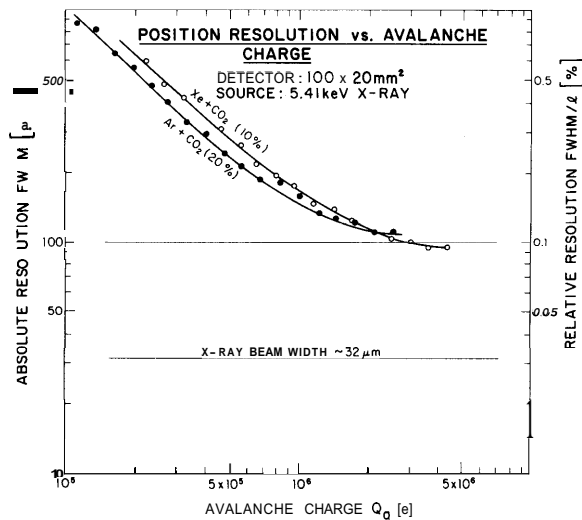


Fig. 4. Position resolution vs anode charge (measured in $1 \mu\text{s}$) for delay line readout detector with active area 10×2 cm², and $1 \mu\text{s}$ delay line.

contemplated. Beyond this point it is really necessary to change readout philosophy, such as described in the next section.

4. Very high counting rate proportional counter

The study of the dynamic structure of biological samples, for example, is made possible by the high photon flux from a synchrotron source. In such experiments the diffraction patterns created by the specimen are recorded in successive time slices which are usually in the range of $100 \mu\text{s}$ to several ms. For such high rate applications it would be very difficult to obtain statistically meaningful data with a delay line readout detector because pulse pileup and dead-time losses would be unmanageably large. Therefore a multielement type of readout is required, for example reading individual anode wires or individual cathode strips. One approach using this solution is to use charge integrating position readout [10]. Although charge integration is capable of dealing with higher absolute counting rates than single photon counting, we have chosen to use the latter because of the larger dynamic range in counting rate inherent to photon counting.

The first detector that we have built for the time resolved studies of biological samples is a one-dimensional chamber with 100 position elements. A side view schematic diagram is shown in fig. 5. It comprises an active area of about $12.7 \times 2 \text{ cm}^2$, with a flat beryllium window. Below the window is a 4 mm deep absorption and drift region, followed by the symmetric structure of a MWPC, with anode cathode spacing 1 mm, and anode wire pitch 1.27 mm. The total chamber depth is thus 6 mm. A wire grid forms the upper cathode, and an aluminum sheet forms the lower cathode. Briefly, the principle is as follows. A photon entering the chamber through the beryllium window creates a small cloud of primary electrons after it has been absorbed in the detector gas. This electron cloud moves along the drift field perpendicular to the plane of the window, drifts through the wire cathode and creates an avalanche on the nearest anode wire. Each anode wire, at ground potential, is connected directly to a preamplifier, followed by a shaping amplifier, discriminator and scaler. The scaler is incremented by one every time an event is recorded by an anode wire whose shaped signal has exceeded the discriminator threshold. All 100 anode channels operate independently and after a time corresponding to one time slice, the contents of the 100 scalers are read (in about 200 ns) into buffer memory, so that the next time slice begins with very little elapsed dead time.

In order that each anode channel can record a significant number of events during one time slice, we have aimed for a counting rate capability in each channel in

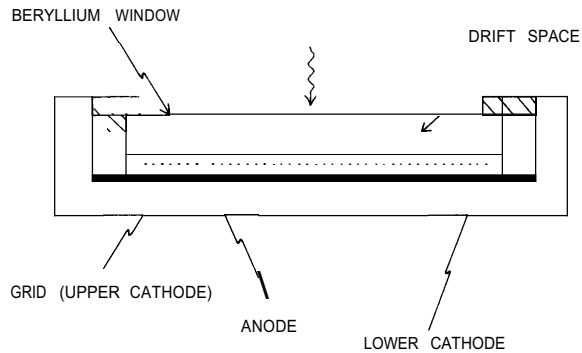


Fig. 5. Schematic diagram of “readout per wire” chamber for very high counting rates ($\approx 10^8 \text{ s}^{-1}$). Drift space is 4 mm deep anode–cathode spacing = 1 mm, anode wire pitch = 1.27 mm (anode wire diameter = $10 \mu\text{m}$), upper cathode wire pitch = 0.635 mm (cathode wire diameter = $50 \mu\text{m}$). Number of anodes = 100. Sensitive area = $12.7 \times 2 \text{ cm}^2$.

excess of 10^6 s^{-1} . Thus the resolving time of each channel should be of the order of 10 ns for dead time losses $\approx 1\%$ (i.e., 5% at $5 \times 10^5 \text{ s}^{-1}$). There are several important factors which have to be satisfied or optimized in order to achieve such performance.

a) The signal induced on an anode wire from an avalanche is due primarily to the drift of positive ions away from the wire. In the chamber described here, 15–20% of the total charge is induced during the first few nanoseconds of ion drift in the high field near the anode (but it takes $\approx 10 \mu\text{s}$ for these ions to finally reach the cathodes). The preamplifier and shaping amplifier integrate this very early part of the induced charge by a fast delay line clipping technique. Pole/zero networks in the shaping amplifier cancel the long tail of the current pulse due to the long positive ion drift time.

b) Independent of the nature of signal shaping employed, there is a natural limitation to counting rate on the same spot of one wire due to “space charge saturation”, in which the creation of too many positive ions reduces the effective field, and hence the gain, at the anode wire. This effect decreases rapidly with decreasing anode–cathode spacing. For this phenomenon not to be a problem at a rates $\approx 10^6 \text{ s}^{-1}$, it is desirable to operate with avalanche sizes no larger than a few $\times 10^5$ electrons. This in turn puts an upper limit on the electronic noise from each channel, otherwise the discriminator threshold cannot be lowered to a value which allows all anode signals to exceed it. The noise from each channel here is ≈ 1500 electrons rms for an input capacitance of $\approx 10 \text{ pF}$, allowing a discrimination threshold around 10^4 electrons. This gives a high sensitivity for signals of a few 10^5 electrons. This technique is described in another high rate application [11] and a full description of the low noise, fast pulse shaping is given in ref. [12].

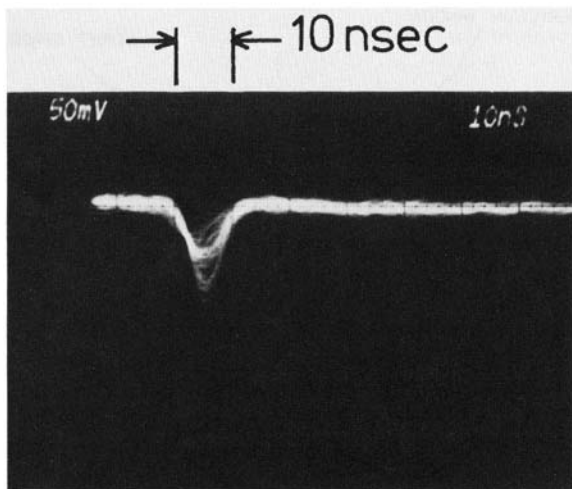


Fig. 6. Waveform from fast shaping amplifier for 5.9 keV X-ray creating avalanche on one wire of the detector in fig. 5. Gas mixture is Xe/5%CO₂/10%CF₄. Recovery time of amplifier \approx 10 ns.

c) A requirement in the chamber amplification process is that the time duration of arrival of the primary ionization, from the X-ray interaction with a gas atom, should be not much longer than the integration time of the shaping amplifier, about 4 ns in this case. There are two main factors which determine this time duration: the size of the primary electron cloud, (directly related to photoelectron range), and the drift velocity of these electrons in the drift section of the detector. Clearly, favorable conditions are a very small electron cloud and high drift velocity. An increase in electron drift velocity can be obtained by addition of CF₄ to xenon [13]. In the present application, we have used a gas mixture of Xe/5%CO₂/10%CF₄ (in which the CO₂ acts as an inorganic quencher to avoid polymerization products associated with organic quenchers). Fig. 6 shows signals from the shaping amplifier for 5.9 keV X-rays with this gas mixture. The waveforms return to the baseline in \approx 10 ns, achieving the required resolving time outlined earlier. Without the increased electron drift velocity provided by CF₄, the signal, for an identical total

avalanche size, is both smaller in height and longer in duration than shown in fig. 6, which leads to loss of counts because of threshold effects, and also to reduced counting rate capability.

Thus, with 100 channels operating in identical but independent fashion, the detector is capable of counting rates in excess of 10^8 s^{-1} with very small dead time losses. A more detailed description of this detector will be given in a future report.

We wish to acknowledge the skills of F. Merritt and E. Von Achen in detector construction and of D. Stephani and L. Rogers in electronic design and testing. A variety of electrodes has been produced in circuit board form by A. De Libero and with thin film vacuum deposition by R. Di Nardo.

References

- [1] G.C. Smith, J. Fischer and V. Radeka, IEEE Trans. Nucl. Sci. NS-31 (1984) 111.
- [2] G.C. Smith, J. Fischer and V. Radeka, IEEE Trans. Nucl. Sci. NS-32 (1985) 521.
- [3] R.A. Boie and V. Radeka, IEEE Trans. Nucl. Sci. NS-27 (1980) 338.
- [4] V. Radeka and R.A. Boie, Nucl. Instr. and Meth. 178 (1980) 543.
- [5] J. Fischer, V. Radeka and G.C. Smith, to be published in IEEE Trans. Nucl. Sci.
- [6] J.E. Bateman, M.W. Waters and R.E. Jones, Nucl. Instr. and Meth. 135 (1976) 235.
- [7] J.E. Bateman and J.F. Connolly, Nucl. Instr. and Meth. 173 (1980) 525.
- [8] R.A. Boie, J. Fischer, Y. Inagaki, F.C. Merritt, V. Radeka, L.C. Rogers and D.M. Xi, Nucl. Instr. and Meth. 201 (1982) 93.
- [9] J. Harder, private communication.
- [10] K. Mochiki and K. Hasegawa, Nucl. Instr. and Meth. A234 (1985) 593.
- [11] J. Fischer, A. Hrisoho, V. Radeka and P. Rehak, Nucl. Instr. and Meth. A238 (1985) 249.
- [12] V. Radeka, A. Hrisoho and D. Stephani, in preparation.
- [13] L.G. Christophorou, D.V. Maxey, D.L. McCorkle and J.G. Carter, Nucl. Instr. and Meth. 171 (1980) 491.